

Decoherence and relaxation of a qubit coupled to an Ohmic bath directly and via an intermediate harmonic oscillator

Xian-Ting Liang

Department of Physics and Institute of Modern Physics, Ningbo University, Ningbo, 315211, China

Abstract

Using the numerical path integral method we investigate the decoherence and relaxation of qubits coupled to an Ohmic bath directly and via an intermediate harmonic oscillator (IHO). Here, we suppose the oscillation frequencies of the bath modes are higher than the IHO's. When we choose suitable parameters the qubits in the two models may have almost same decoherence and relaxation times. However, the decoherence and relaxation times of the qubit in the qubit-IHO-bath model can be modulated through changing the coupling coefficients of the qubit-IHO and IHO-bath and the oscillation frequency of the IHO.

PACS numbers: 67.57.Lm, 03.65.Yz, 31.15.Kb

I. INTRODUCTION

Since Shor's algorithm [1] for factoring large numbers, the theory of quantum computation and quantum information has attracted great recent interest. It is believed that quantum computers may perform some useful tasks more efficiently than their classical counterparts. Despite the great promises of performing quantum computations, however, there are still many practical difficulties to be resolved before quantum computers might become available in future. One of the difficulties is that the qubit has too short decoherence time, which is in fact a central impediment for practical qubit to be taken as the cell of quantum computers. Solid-state qubits are considered to be promising candidates for realizing building blocks of quantum computers because of their integrability and flexibility in the design. However, the quantum logical gates or registers made up with these qubits have still shorter decoherence and relaxation times. These motivated a lot of studies on the decoherence, relaxation and manipulation of the qubits. Many significant results in the field, not only theoretical but also experimental, have been achieved. Most of the theoretical research is based on a spin-boson (SB) model which is supposed to be constructed with a spin (qubit or two-level system) coupled to a bath. The model has many physical correspondences and has been widely investigated in recent years [2, 3, 4]. In order to investigate a qubit in its environment, there is another model which is different from the original spin-boson one. In the model, the qubit couples to the coordinate X of a harmonic oscillator, which we shall sometimes call the "intermediate harmonic oscillator" (IHO), and which in turn is coupled to a bath. We call the model the spin-IHO-bath (SIB) model. Recently, this model receives much interest in the context of quantum computing with condensed matter systems, especially with superconducting flux qubit devices, see Ref. [5] and within. It is also useful to investigate the measurement of the solid-state qubit [6] and magnetic resonance force microscopy [7, 8].

On the other hand, the SB and SIB models can be used

to describe the electron transfer in chemical and biological molecules. Many theoretical investigations in this field use the SB model [9, 10, 11, 12]. Based on Leggett [13], Garg *et al.* [14] investigated the SIB model, and obtained a map of it to the SB one, and obtained the spectral density of the effective bath for the map. They used this model to study the migration of an electron from one biomolecule to another, or between two localized sites in the same biomolecule. It has been shown that the coherence is very important not only to qubits for making quantum computers but also to electrons for transferring energy in biological systems [15, 16]. However, if one wants to know the decoherence and relaxation behaviors of the two-level systems in their environment, essentially, the dynamics of the systems needs to be known.

If the qubit energy splitting (denoted by Δ hereinafter) is not equal to zero, the two models are not exactly solvable. However, they can be analyzed using adiabatic renormalization in which a systematic weak damping approximation must be used. They can also be investigated with some approximation methods based on the perturbative scheme which also asks for the systems (qubits) weakly coupling to their environment. Many other methods [17, 18, 19] for solving the models have been proposed in recent years, most of which are based on the Born-Markov approximation. However, it has been pointed out that the use of the approximation is inappropriate at the large tunneling amplitude and low temperatures. Recently, some different schemes to solve the SIB model have also been put forward. Gassmann *et al.* [8] obtain an exactly solvable model from the SIB through dropping an unimportant term, where an approximation similar to the Born-Oppenheimer one is used. This method is not successful as the "dropping term" is not small enough. So it is important to find out some methods to accurately estimate the dynamics of the qubits in the two models. Based on the insight into the dynamics we may understand the decoherence and relaxation better and may bring forward some schemes on how to suppress them. It is also of much interested to find out the qubit in which model, SB or SIB, has longer decoherence and relaxation times. These problems are not obvious.

An excellent method, accurate numerical path integral method based on the quadiabatic propagator path integral (QUAPI) scheme [20, 21] may be a suitable tool for solving the two models. To our problems we choose the iterative tensor multiplication (ITM) algorithm for the numerical scheme. As Makri [20, 21] addressed that the method is non-Markovian and it can make the calculations accurate enough even at very low temperatures, large tunneling amplitude and strong couplings for which the Markovian approximation is unsuitable. In this paper we shall use the tool to investigate the dynamics and then the decoherence and relaxation of the qubit in the SB and SIB models.

II. MODELS AND DYNAMICS

The Hamiltonian of the SB model is

$$H_{SB} = \hbar \left(\frac{\epsilon}{2} \sigma_z + \frac{\Delta}{2} \sigma_x \right) + \sum_i \left[\frac{p_i^2}{2m_i} + \frac{1}{2} m_i \omega_i^2 \left(x_i + \frac{c_i \sigma_z}{m_i \omega_i^2} \right)^2 \right] \quad (1)$$

Suppose the bath has an Ohmic spectral density

$$J_{ohm}(\omega) = \frac{\pi}{2} \sum_i \frac{c_i^2}{m_i \omega_i} \delta(\omega - \omega_i) = \frac{\pi}{2} \hbar \xi \omega e^{-\omega/\omega_c}. \quad (2)$$

Here, ξ is the dimensionless Kondo parameter [12, 22] (the relationship of ξ with the friction coefficient η is $\xi = 2\eta/\pi\hbar$ [23]), σ_i ($i = x, z$) are the Pauli matrix, and ω_c is the high-frequency cutoff of the bath modes. This is a well-known quantum dissipation model and it has been widely investigated [2, 3].

If we consider the qubit coupling to the coordinate X of a single IHO which in turn is coupled to a bath, and if we let the couplings be linear, the Hamiltonian of the SIB system reads

$$H_{SIB} = \hbar \left(\frac{\epsilon}{2} \sigma_z + \frac{\Delta}{2} \sigma_x \right) + \frac{P^2}{2M} + \frac{1}{2} M \Omega_0^2 (X + \lambda \sigma_z)^2 + \sum_i \left[\frac{p_i^2}{2m_i} + \frac{1}{2} m_i \omega_i^2 \left(x_i + \frac{\kappa c_i X}{m_i \omega_i^2} \right)^2 \right], \quad (3)$$

where M and P are the mass and momentum of the IHO, and the displacement λ characterizes the coupling of the qubit to the IHO, and κc_i are the coupling coefficients of the IHO to the bath modes. It is shown that the system has a one to one map to the following system [14]

$$H_{SIB} = \hbar \left(\frac{\epsilon}{2} \sigma_z + \frac{\Delta}{2} \sigma_x \right) + \sum_i \left[\frac{\tilde{p}_i^2}{2\tilde{m}_i} + \frac{1}{2} \tilde{m}_i \tilde{\omega}_i^2 \left(\tilde{x}_i + \frac{\tilde{c}_i \sigma_z}{\tilde{m}_i \tilde{\omega}_i^2} \right)^2 \right] \quad (4)$$

with an effective spectral density (see Appendix)

$$\begin{aligned} J_{eff}(\omega) &= \frac{\pi}{2} \sum_i \frac{\tilde{c}_i^2}{\tilde{m}_i \tilde{\omega}_i} \delta(\omega - \tilde{\omega}_i) \\ &= \frac{\pi}{2} \lambda^2 \kappa^2 \xi \hbar \omega \frac{\Omega_0^4}{(\omega^2 - \Omega_0^2)^2 + 4\Gamma^2 \omega^2}, \end{aligned} \quad (5)$$

where $\Gamma = \kappa^2 \eta / 2M$. When the bath modes have lower frequencies than Ω_0 , the dynamics of the qubit in the bath with effective spectral density $J_{eff}(\omega)$ is similar to the dynamics of the qubit in Ohmic bath with spectral density $J_{ohm}(\omega)$, which is widely investigated in recent years [24, 25, 26, 27, 28, 29, 30]. In this paper we investigate another limited case, namely, the bath modes have higher frequencies than the oscillation frequency Ω_0 of IHO. The length of the memory times of the baths can be estimated by the following bath response function

$$\alpha(t) = \frac{1}{\pi} \int_0^\infty d\omega J(\omega) \left[\coth\left(\frac{\beta \hbar \omega}{2}\right) \cos \omega t - i \sin \omega t \right]. \quad (6)$$

Here, $\beta = 1/k_B T$ where k_B is the Boltzmann constant, and T is the temperature. It is shown that when the real and imaginary parts behave as the delta function $\delta(t)$ and its derivative $\delta'(t)$, the dynamics of the reduced density matrix is Markovian. However, if the real and imaginary parts are broader than the delta function, the dynamics is non-Markovian. The broader the $\text{Re}[\alpha(t)]$ and $\text{Im}[\alpha(t)]$ are, the longer the memory time will be. The broader the $\text{Re}[\alpha(t)]$ and $\text{Im}[\alpha(t)]$ are, the more serious the practical dynamics will be distorted by the Markovian approximation. The memory time of the effective bath is determined by Γ . The larger the Γ is, the shorter the memory time of the effective bath will be. If the memory time of the bath is short enough, the reduced density matrix may be obtained in virtue of the Markovian approximation. However, if the memory time of the bath is too long, the ITM method is in fact inappropriate, saying nothing of other methods based on Markovian approximation. Clearly, the value of the Γ may vary according to the difference of the physical systems. For example, when the persistent-current qubit is measured by a dc SQUID, the system can be modeled by Eq. (4) with Eq. (5), here $\Gamma = 1/R_s C_s$. Typically, $R_s = 100 \Omega$, $C_s = 5$ pF, so $\Gamma \sim 10^{11}$, see Ref. [29]. In this paper we set $\Gamma = 2.6 \times 10^{11}$. This value of Γ makes the calculation with ITM suitable but other methods based on Markovian approximation unsuitable.

In Fig. 1 we plot the $\text{Re}[\alpha(t)]$ and $\text{Im}[\alpha(t)]$ as $J(\omega) = J_{ohm}(\omega)$, and $J_{eff}(\omega)$, where we set $\lambda \kappa = 1050$, $\xi = 0.01$, $\Omega_0 = 10\Delta$, $T = 0.01$, $\Gamma = 2.6 \times 10^{11}$, $\Delta = 5 \times 10^9$ Hz, the lower-frequency and high-frequency cut-off of the baths modes $\omega_0 = 11\Delta$, and $\omega_c = 100\Delta$. It is shown that the memory time of the Ohmic bath is similar to the one of the effective bath, namely, $\omega_c \tau_{SB}^m \sim \omega_c \tau_{SIB}^m$. Both baths have shorter effective memory times. This will be verified in Fig. 2 below.

The dynamics of the qubit is characterized by the time evolution of the reduced density matrix, obtained after tracing out the bath degrees of freedom, i.e.,

$$\rho(s'', s'; t) = \text{Tr}_{bath} \langle s'' | e^{-i\mathcal{H}t/\hbar} R(0) e^{i\mathcal{H}t/\hbar} | s' \rangle. \quad (7)$$

In actual cases the initial state of the total system must be entangled even at the beginning of the evolution. However, at the beginning the entanglement is very weak,

otherwise the qubit must have lost its coherence and relaxed to its thermal equilibrium in a very short time. This is not our case investigated in this paper. So, for simplicity of the presentation we assume that the entanglement (through interaction) between the qubit and its environment is switched on at $t = 0$, i.e., the initial density matrix has the form [12, 20, 21, 22, 23]

$$R(0) = \rho(0) \otimes \rho_{bath}(0), \quad (8)$$

where $\rho(0)$ and $\rho_{bath}(0)$ are the initial states of the qubit and bath. The scheme which we use to calculate the reduced density matrix $\rho(t)$ is a well established ITM algorithm derived from the QUAPI. It is a numerically exact algorithm and is successfully tested and adopted in various problems of open quantum systems [12, 22, 23]. For details of the scheme, we refer to previous works [20, 21]. The QUAPI asks for the system Hamiltonian splitting into two parts H_0 and H_{env} . Here, we take $H_0 = \hbar(\frac{\epsilon}{2}\sigma_z + \frac{\Delta}{2}\sigma_x)$ and $H_{env} = H_{SB} - H_0$, or $H_{env} = H_{SIB} - H_0$. In order to make the calculations converge we use the time step $\omega_c \Delta t = 0.6$, which is smaller than the characteristic times of the qubits in the systems.

III. DECOHERENCE AND RELAXATION

The decoherence is in general produced due to the interaction of the quantum system with other systems with a large number of degrees of freedom, for example the devices of the measurement or environment. To measure the decoherence one may use the entropy, the first entropy, and many other measures, such as the maximal deviation norm, etc. (see for example Refs. [31, 32, 33]). However, essentially, the decoherence of an open quantum system is reflected through the decays of the off-diagonal coherent terms of its reduced density matrix [34]. The decoherence time denoted by τ_2 measures the time of the initial coherent terms to their $1/e$ times, namely, $\rho_i(n, m) \xrightarrow{\tau_2} \rho_f(n, m) = \rho_i(n, m)/e$. Here, $n \neq m$, and $n, m = 0$ or 1 for qubits. In the following, we investigate the decoherence via directly describing the evolutions of the off-diagonal coherent terms, instead of using any measure of the decoherence. Similar to the decoherence, the relaxation of the qubit can also be investigated with the diagonal elements of the reduced density matrix. The relaxation time is denoted by τ_1 , which measures the time of an initial state to the final thermal equilibrium state through estimating the diagonal terms of the reduced density matrix, namely, $\rho_i(n, n) \xrightarrow{\tau_1} e^{-E_n/k_b T}$. In the following calculations we assume the initial state of the environment $\rho_{bath}(0) = \prod_k e^{-\beta M_k} / \text{Tr}_k(e^{-\beta M_k})$. As calculating the off-diagonal element ρ_{12} we let $\epsilon = 10\Delta$ which can make the ρ_{12} decay stably. If $\epsilon \rightarrow \Delta$ the ρ_{12} will decay with some oscillations, which may affect our judgement on decoherence times. The closer the two parameters are, the more strongly the matrix elements will oscillate. When

we calculate ρ_{11} we choose parameters $\epsilon = \Delta$ because the oscillations of the ρ_{11} do not affect our judgement on relaxation times from the figures. The reader should note that, the increase of the Δ and ϵ will shorten the decoherence and relaxation times, so the decoherence time τ_2 and the relaxation time τ_1 in the figures are not comparable because they are plotted in different two sets of the parameters. But, it is clear that the relaxation time τ_1 is longer than the decoherence time τ_2 .

In the ITM scheme, one should at first choose the k_{\max} , so that $k_{\max}\omega_c\Delta t$ must be larger than the effective memory time $\omega_c\tau_{SB}^m$ and $\omega_c\tau_{SIB}^m$ of the baths. In Fig. 2 we plot the reduced density matrix elements ρ_{11} and ρ_{12} as $k_{\max} = 2, 3$, and 4 for the SB and SIB models. Here, we set $\lambda\kappa = 1050$, the low- and high-frequency cut-off are $\omega_0 = 11\Delta$, and $\omega_c = 100\Delta$. From the Fig. 2 we obtain that as $\lambda\kappa = 1050$ the qubit has almost the same decoherence and relaxation times in SB and SIB models, and the calculations are in fact convergent as $k_{\max} \geq 3$. It is known that the qubit will show different decoherence and relaxation when it has different initial states. We can not obtain general results on the decoherence and relaxation from some special initial states. Essentially, this limitation is inevitable, because in order to obtain measures of the decoherence and relaxation one should perform the calculations over all possible initial states in general [30, 31]. But, we may figure out some information on the trend of the decoherence and relaxation of the qubit from some special results. In particular, we are more interested in some special results because some schemes on quantum information are based on the usage of some special initial states. In Fig. 3 we plot the decoherence and the relaxation of the qubit in SB (a) and SIB (b) models in different initial states. These states are $|\xi_1\rangle = [\sqrt{1/2}, \sqrt{1/2}]^T$, $|\xi_2\rangle = [\sqrt{3/4}, \sqrt{1/4}]^T$, $|\xi_3\rangle = [\sqrt{6/7}, \sqrt{1/7}]^T$, $|\xi_4\rangle = [\sqrt{12/13}, \sqrt{1/13}]^T$, $|\xi_5\rangle = [\sqrt{29/30}, \sqrt{1/30}]^T$, $|\xi_6\rangle = [\sqrt{59/60}, \sqrt{1/60}]^T$, $|\xi_7\rangle = [1, 0]^T$. As $\lambda\kappa > 1050$ (or $\lambda\kappa < 1050$) the decoherence and relaxation times will be shortened (or lengthened), as shown in Fig. 4. The frequency of the IHO will strongly affect the qubit decoherence and relaxation. If the Ω_0 of the IHO decreases, the decoherence and relaxation times will be lengthened, and vice versa. Namely, the farther the Ω_0 departs from the lower-frequency cut-off of the bath, the longer decoherence and relaxation times the qubit will have, as evidenced in Fig. 5.

IV. CONCLUSIONS

In this Letter we have investigated the decoherence and relaxation of a qubit coupled to an Ohmic bath directly and via an IHO. In our investigations, we fix the tunneling splitting Δ of the qubit and assume that the IHO is far off the resonance to the environment modes, i.e.

the oscillation frequency of the IHO is smaller than the lower-frequency cut-off of the bath modes. In addition, we suppose that the damping coefficient Γ of a bath to the IHO is moderate. If the quantity is too small, the memory time of the bath may be very long, thus the methods based on not only the Markovian approximation but also the ITM scheme are inappropriate for the investigation of the qubit dynamics. On the contrary, if the Γ is too large, and the memory effects of the bath can be neglected, the dynamics of the qubit can be investigated in many other ways based on the Markovian approximation. In spite of these limitation our investigations have wider appeal because the method is suitable for a wider range of Γ , and most practical physical systems have the moderate Γ . By use of the accurate numerical path integral scheme, the ITM based on the QUAPI method we have obtained the evolutions of the reduced density matrix elements of qubit in the SB and SIB models. We have obtained that: (1) When $\lambda\kappa = 1050$ the qubit in the SIB model has almost the same decoherence and relaxation times with the qubit in the SB model. If $\lambda\kappa > 1050$ the damping of a bath to the IHO or (and) the IHO to the qubit increase, which results in the decrease of the decoherence and relaxation times, and vice versa. (2) The decoherence and relaxation times of the qubit in the SIB model increase with the decrease of the oscillation frequency Ω_0 of the IHO, and vice versa. (3) The decoherence and relaxation times of the qubit in the SB and SIB models will increase with the decrease of the ϵ and Δ , which has not been plotted in the Letter. The longer decoherence and relaxation times are necessary for not only the qubits for making the quantum computers but also the electrons for transferring energy in biological systems. In order to make the qubits or electrons in the SIB model have longer decoherence and relaxation times we may try to make the Ω_0 and $\lambda\kappa$ smaller.

Acknowledgement 1 *This project was sponsored by National Natural Science Foundation of China (Grant No. 10675066) and K.C.Wong Magna Foundation in Ningbo University.*

V. APPENDIX

In the appendix we derive the effective spectral density expressed with Eq. (5). As Ref. [14] pointed out that the map from Eq. 3 to Eq. 4 does not involve the spin (qubit), the same $J_{eff}(\omega)$ will control the dynamics of a continuous variable q moving in some potential $U(q)$ and coupled to coordinates X and $\{x_i\}$ in the same way as the spin. So we can deduce the $J_{eff}(\omega)$ with the Hamiltonian

$$H = \frac{p_q^2}{2\mu} + U(q) + \frac{P^2}{2M} + \frac{1}{2}M\Omega_0^2(X + \lambda q)^2 + \sum_i \left[\frac{p_i^2}{2m_i} + \frac{1}{2}m_i\omega_i^2 \left(x_i + \frac{\kappa c_i X}{m_i\omega_i^2} \right)^2 \right], \quad (9)$$

where p_q is the momentum conjugate to q . Defining $U' = dU/dt$ and using the dots for the time derivatives, the classical equations of the motion are

$$\mu\ddot{q} = -U'(q) - M\Omega_0^2(X + \lambda q)\lambda, \quad (10)$$

$$M\ddot{X} = -M\Omega_0^2(X + \lambda q) - \sum_i \kappa c_i x_i - X \sum_i \frac{\kappa^2 c_i^2}{m_i \omega_i^2}, \quad (11)$$

$$m_i \ddot{x}_i = -m_i \omega_i^2 x_i - \kappa c_i X. \quad (12)$$

Using the Fourier transforms, Eqs. (10-12) can be written as

$$(-\mu\omega^2 + M\Omega_0^2\lambda^2)q(\omega) + M\Omega_0^2X(\omega)\lambda = -U'_\omega(q), \quad (13)$$

$$\left(-M\omega^2 + M\Omega_0^2 + \sum_i \frac{\kappa^2 c_i^2}{m_i \omega_i^2} \right) X(\omega) + \sum_i \kappa c_i x_i(\omega) = -M\Omega_0^2\lambda q(\omega), \quad (14)$$

$$x_i(\omega) = -\frac{\kappa c_i}{m_i(\omega_i^2 - \omega^2)} X(\omega). \quad (15)$$

Insetting Eq. (15) into Eq. (14), we have

$$\left(-M\omega^2 + M\Omega_0^2 - \omega^2 \sum_i \frac{\kappa^2 c_i^2}{m_i \omega_i^2 (\omega_i^2 - \omega^2)} \right) X(\omega) = -M\Omega_0^2\lambda q(\omega). \quad (16)$$

Using the notation

$$L(\omega) = -\omega^2 \left(M + \sum_i \frac{\kappa^2 c_i^2}{m_i \omega_i^2 (\omega_i^2 - \omega^2)} \right), \quad (17)$$

and Eq. (16) we have

$$X(\omega) = \frac{-M\Omega_0^2\lambda q(\omega)}{M\Omega_0^2 + L(\omega)}. \quad (18)$$

Insetting Eq. (18) into Eq. (13), we have

$$\left\{ -\mu\omega^2 + \frac{M\Omega_0^2\lambda^2 [M\Omega_0^2 + L(\omega)]}{M\Omega_0^2 + L(\omega)} - \frac{(M\Omega_0^2)^2 \lambda^2}{M\Omega_0^2 + L(\omega)} \right\} q(\omega) = -U'_\omega(q). \quad (19)$$

Introducing the function $K(\omega)$, and making

$$K(\omega)q(\omega) \equiv \left[-\mu\omega^2 + \frac{M\Omega_0^2\lambda^2 L(\omega)}{M\Omega_0^2 + L(\omega)} \right] q(\omega) = -U'_\omega(q). \quad (20)$$

By using Eqs. (2) and (16) we have

$$\begin{aligned} L(\omega) &= -\omega^2 \left(M + \kappa^2 \int_0^\infty \frac{1}{\omega'(\omega'^2 - \omega^2)} \right. \\ &\quad \left. \times \sum \frac{c_i^2}{m_i \omega_i} \delta(\omega' - \omega_i) d\omega' \right) \\ &= -\omega^2 \left(M + \frac{2\kappa^2 \pi}{\pi} \int_0^\infty \frac{J_{ohm}}{\omega'(\omega'^2 - \omega^2)} d\omega' \right) \\ &= -\omega^2 \left(M + \frac{2\kappa^2 \eta}{\pi} \int_0^\infty \frac{\exp(-\omega'/\omega_c)}{\omega'(\omega'^2 - \omega^2)} d\omega' \right) \\ &= -M\omega^2 + i\eta\kappa^2\omega e^{-\omega/\omega_c}. \end{aligned} \quad (21)$$

Taking the cut-off frequency to be infinity, we have

$$L(\omega) = -M\omega^2 + i\eta\kappa^2\omega. \quad (22)$$

Substituting this in Eq. (20), from $J_{eff}(\omega) = \lim_{\epsilon \rightarrow 0^+} \text{Im}[K(\omega - i\epsilon)]$ (ω is real), we have

$$J_{eff}(\omega) = \frac{\pi}{2} \lambda^2 \kappa^2 \xi \hbar \omega \frac{\Omega_0^4}{(\omega^2 - \Omega_0^2)^2 + 4\Gamma^2 \omega^2}. \quad (23)$$

Here, $\Gamma = \kappa^2 \eta / 2M$, and $\xi = 2\eta / \pi \hbar$.

-
- [1] P. W. Shor, SIAM J. Sci. Statist. Comput. 26 (1997) 1484.
- [2] U. Weiss, *Quantum Dissipative Systems*, 2nd ed., (World Scientific Publishing, Singapore, 1999).
- [3] A. J. Leggett, S. Chakravarty, A. T. Dorsey, M. P. A. Fisher, A. Garg, and W. Zwerger, Rev. Mod. Phys. 59 (1987) 1.
- [4] A. O. Caldeira and A. J. Leggett, Ann. Phys. (N. Y) 149 (1983) 374.
- [5] M. Thorwart, E. Paladino, and M. Grifoni, Chem. Phys. 296 (2004) 333.
- [6] F. K. Wilhelm, Phys. Rev. B 68 (2003) 060503(R).
- [7] D. Rugar, B. Budakian, H. J. Mamin, and B. W. Chui, Nature 430 (2004) 329.
- [8] H. Gassmann, M.-S. Choi, H. Yi, and C. Bruder, Phys. Rev. B 69 (2004) 115419.
- [9] B. Balzer, and G. Stock, Chem. Phys. 310 (2005) 33.
- [10] L. Muhlbacher, and R. Egger, J. Chem. Phys. 118 (2003) 179.
- [11] J. Ray, and N. Makri, J. Phys. Chem. A 103 (1999) 9417.
- [12] N. Makri, and D. E. Makarov, J. Chem. Phys. 102 (1995) 4600.
- [13] A. J. Leggett, Phys. Rev. B 30 (1984) 1208.
- [14] A. Garg, J. N. Onuchic, and V. Ambegaokar, J. Chem. Phys. 83 (1995) 4491.
- [15] G. S. Engel, T. R. Calhoun, E. L. Read, T. -K. Ahn, T. Mančal, Y. -C. Cheng, R. E. Blankenship, and G. R. Fleming, Nature 446 (2007) 782.
- [16] H. Lee, Y. -C. Cheng, and G. R. Fleming, Science 316 (2007) 1462.
- [17] K. Shiokawa, and B. L. Hu, Phys. Rev. A 70 (2004) 062106.
- [18] Y. Makhlin, G. Schon, and A. Shnirman, Chem. Phys. 296 (2004) 315.
- [19] N. V. Prokof'ev, and P. C. E. Stamp, Rep. Prog. Phys. 63 (2000) 669.
- [20] D. E. Makarov and N. Makri, Chem. Phys. Lett. 221 (1994) 482.
- [21] N. Makri, J. Math. Phys. 36 (1995) 2430.
- [22] N. Makri and D. E. Makarov, J. Chem. Phys. 102 (1995) 4611.
- [23] K. Dong and N. Makri, Phys. Rev. A 70 (2004) 042101.
- [24] M. Thorwart, M. Grifoni, and P. Hanggi, Ann. Phys. (N. Y) 293 (2001) 15.
- [25] M. C. Goorden, M. Thorwart, and M. Grifoni, Phys. Rev. Lett. 93 (2004) 267005.
- [26] M. Thorwart, L. Hartmann, I. Goychuk, and P. Hänggi, J. Mod. Opt. 47 (2000) 2905.
- [27] M. C. Goorden, M. Thorwart, and M. Grifoni, Eur. Phys. J. B 45 (2005) 405.
- [28] M. Thorwart, and P. Hanggi, Phys. Rev. A 65 (2001) 012309.
- [29] L. Tian, S. Lloyd, and T. P. Orlando, Phys. Rev. B 65 (2002) 144516.
- [30] M. J. Storcz, U. Hartmann, S. Kohler, and F. K. Wilhelm, Phys. Rev. B 72 (2005) 235321.
- [31] V. Privman, J. Stat. Phys. 110 (2003) 957.
- [32] L. Fedichkin, A. Fedorov, Phys. Rev. A 69 (2004) 032311.
- [33] L. Fedichkin, A. Fedorov and V. Privman, Phys. Lett. A 328 (2004) 87.
- [34] X. -T. Liang, Phys. Rev. B 72 (2005) 245328.

VI. FIGURE CAPTIONS

Fig. 1 The response functions of the Ohmic bath and effective bath, where $\Delta = 5 \times 10^9$ Hz, $\lambda\kappa = 1050$, $\xi = 0.01$, $\Omega_0 = 10\Delta$, $T = 0.01$, $\Gamma = 2.6 \times 10^{11}$, the lower-frequency and high-frequency cut-off of the baths modes $\omega_0 = 11\Delta$, and $\omega_c = 100\Delta$.

Fig. 2 The evolutions of reduced density matrix elements ρ_{12} and ρ_{11} in SB and SIB models in different values of K_{\max} . Here, $\epsilon = 10\Delta$ for ρ_{12} , $\epsilon = \Delta$ for ρ_{11} , the initial state is $|\xi_1\rangle$ and the other parameters are the same as in Fig. 1.

Fig. 3 The evolutions of reduced density matrix elements of ρ_{12} and ρ_{11} in SB (a) and SIB (b) models in different initial states. These initial states are given in the context. Here, $K_{\max} = 3$, and the other parameters are the same as in Fig. 2.

Fig. 4 The evolutions of reduced density matrix elements of ρ_{12} and ρ_{11} in SIB model in different values of $\kappa\lambda$, the other parameters are the same as in Fig. 2.

Fig. 5 The evolutions of reduced density matrix elements of ρ_{12} and ρ_{11} in SIB model in different values of Ω_0 , the other parameters are the same as in Fig. 2.

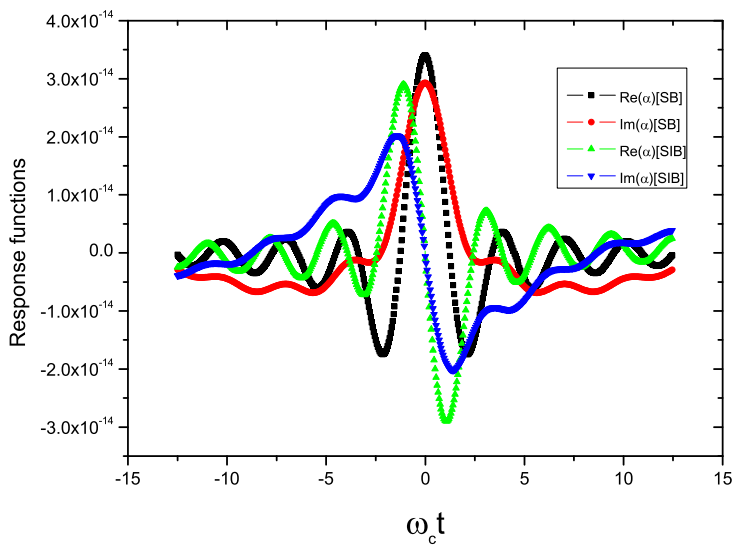


Fig.1

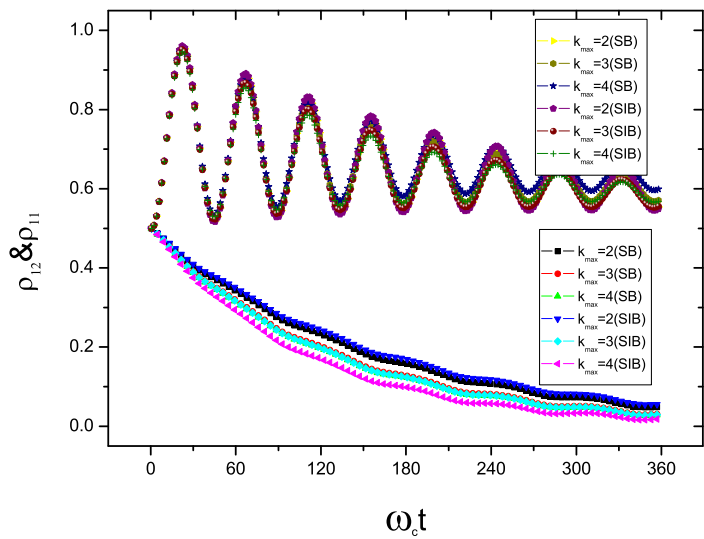


Fig.2

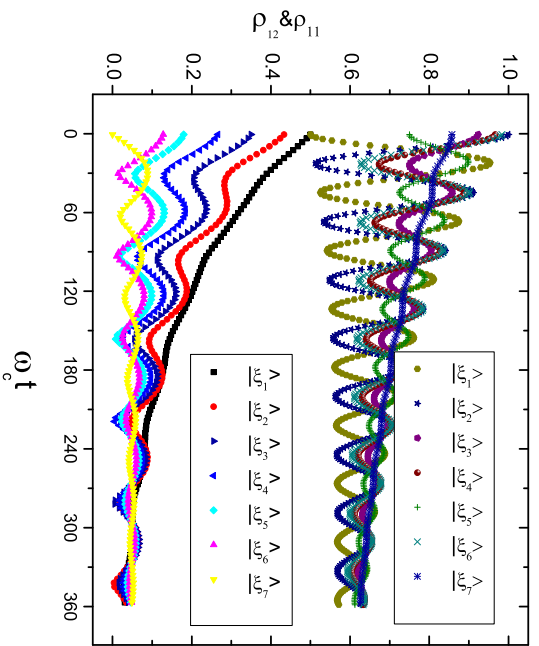


Fig.3a

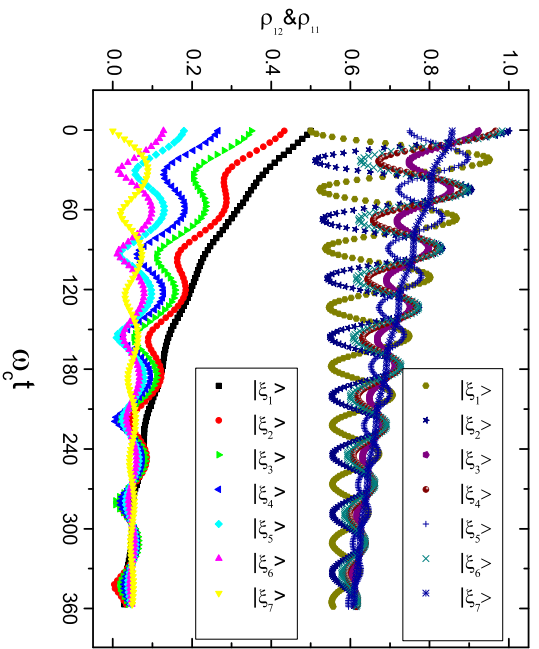


Fig. 3b

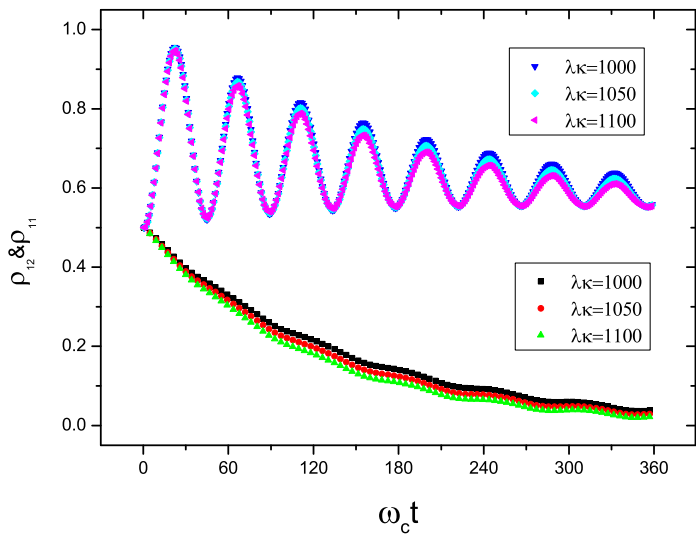


Fig.4

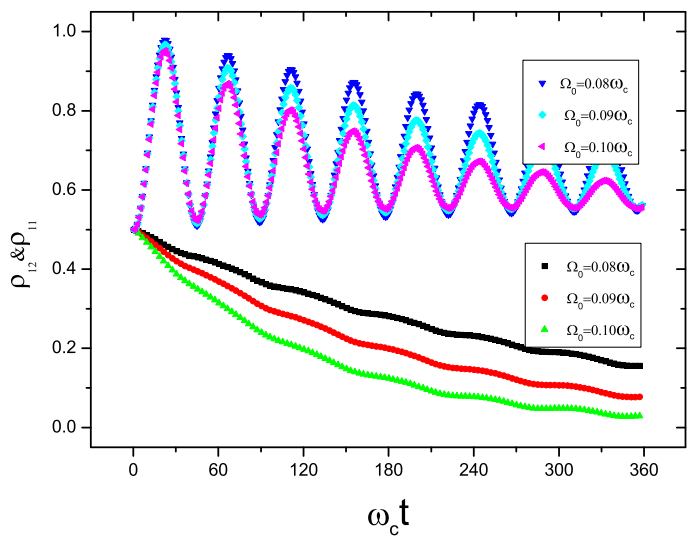


Fig.5